Search for fission from a long-lived isomer in ^{250}No and evidence of a second isomer

J. Khuyagbaatar,[1,2,*] H. Brand,[2] Ch. E. Düllmann,[1,2,3] F. P. Heßberger,[1,2] E. Jäger,[2] B. Kindler,[2] J. Krier,[2] N. Kurz,[2] B. Lommel,[2] Yu. Nechiporenko,[4,5] Yu. N. Novikov,[4,5] B. Schausten,[2] and A. Yakushev[2]

[1]*Helmholtz-Institut Mainz, 55099 Mainz, Germany*
[2]*GSI Helmholtzzentrum für Schwerionenforschung, 64291 Darmstadt, Germany*
[3]*Johannes Gutenberg-Universität Mainz, 55099 Mainz, Germany*
[4]*St. Petersburg State University, St. Petersburg, 199034, Russia*
[5]*Petersburg Nuclear Physics Institute, NRC "Kurchatov Institute", Gatchina, Leningrad Region, 188300, Russia*

(Received 28 June 2022; accepted 26 July 2022; published 5 August 2022)

In the present work, a K isomeric state in ^{250}No, which is more stable against fission than the ground state, was experimentally studied. The aim was to measure the fission branch of this isomeric state. In total, 780 fission events attributed to the decay of ^{250}No were detected. Among them 133 cases were attributed to the ground-state decay with a half-life of 4.0(4) μs, which was populated by the deexcitation of the isomeric state via electromagnetic transitions with a half-life of 23(4) μs. In addition, in two more cases, this long-lived isomeric state was populated in the deexcitation of a hitherto unknown, yet higher-lying and short-lived isomeric state with a half-life of $0.7^{+1.4}_{-0.3}$ μs. No direct fission from the long-lived isomeric state, i.e., with a lifetime of longer than 40 μs, was identified. This results in an upper limit of 0.035 for the branching ratio for fission. This is a significantly more strict limit than the previously known value of 0.5. Nonobservation of fission branching of the long-lived isomer is discussed relative to theoretical predictions and within various semiempirical ways, which resulted in an attribution of a lower limit of 10^4 for the fission-hindrance factor, caused by the K quantum number. The presences of multiple high-K isomeric states seemingly is a widespread phenomenon in deformed heavy nuclei.

DOI: 10.1103/PhysRevC.106.024309

I. INTRODUCTION

In the last two decades, many isomeric states have been discovered and studied in the region of deformed heavy nuclei with proton and neutron numbers around $Z = 100$ and $N = 152$, respectively [1]. Among these, so-called K-isomeric states, which are formed by coupling of up to several quasiparticles, are of special interest [2–5]. Because of quantum selection rules for the K quantum number, which is the projection of the total spin of the nucleus onto the axial symmetry axis, decay of a high-K state by electromagnetic transitions may be strongly hindered [5,6]. In turn, the coupling of quasiparticles can also hinder the spontaneous fission process [7–10].

As consequences of such hindrances, it may occur in heavy nuclei that fission from a high-K state is strongly retarded compared to that from the ground state, despite a high excitation energy, which should favor fission. In other words, the K-isomeric state may have a partial fission half-life longer than that of the ground state [9]. However, this does not necessarily mean that such an excited high-K state would live longer than the ground state, because it may still decay via electromagnetic transitions and/or by α decay [1–3,5,11,12]. The competition between these decay modes is governed by physical quantities that characterize the properties of an individual nucleus, e.g., the fission barrier, the K quantum number, excitation energy, the level density, etc.

Nevertheless, in three nuclei (^{270}Ds [13], ^{250}No [14–16], and ^{254}Rf [17]) high-K isomeric states that are more stable than the respective ground states have been identified. Therefore, K-isomeric states, which have extra stability that retards fission, are an intriguing topic in both experimental and theoretical studies of the heaviest nuclei. The effect of the K number on fission can theoretically be described within various models [8–10]. Their results are often represented as an increase of the fission-barrier height compared to that of the ground state. Such results, indeed, qualitatively describe the enhanced stability of the isomeric state against fission. However, for a quantitative description of the properties of the K-isomeric state, more complete experimental data, e.g., fission half-lives of both isomeric and ground states in a particular nucleus, are needed.

In the above mentioned three nuclei, direct fission of the isomeric states, which would allow one to quantify the fission hindrance of isomeric states due to their high-K quantum numbers, has not yet been observed.

For a long time, fission events with two half-lives of $\approx$3.8 μs [16] and $\approx$34.9 μs [16] were known to occur in ^{250}No [14–16]. Only recently, experimental evidence has been obtained which showed that the long-lived fission activity originates from the decay of a high K-isomeric state, which

*J.Khuyagbaatar@gsi.de

deexcites via electromagnetic transitions to the short-lived spontaneously fissioning ground state [16]. A direct fission from the isomeric state has not been identified and only an upper limit of 0.5 for the fission branch was given, which led to the conclusion that the probability of the isomeric state to undergo fission is at least 19 times smaller than that of spontaneous fission of the ground state [16]. This boundary value, which indicates a large hindrance, however, does not allow one to elucidate the full strength and impact of the K quantum number on the fission process. Therefore, the measurement of the fission branch of the long-lived isomeric state of ^{250}No is still an important experimental topic in the field.

In the present work, we studied the decay of ^{250}No using fast digital electronics, in which the sensitivity also for the detection of conversion electrons (CEs) originating from the deexcitation of K-isomeric states was shown to be very high [18].

II. EXPERIMENTAL SETUP

The experiment was performed at the gas-filled Trans-Actinide Separator and Chemistry Apparatus (TASCA) at GSI, Darmstadt, Germany [19] in 2018. A pulsed (5-ms-long pulses, ≈ 5/s repetition rate) ^{48}Ca^{10+} beam was accelerated by the Universal Linear Accelerator UNILAC to 218.9 MeV. Lead targets (isotopic composition: 99.94% ^{204}Pb; 0.04% ^{206}Pb; 0.01% ^{207}Pb; 0.01% ^{208}Pb) with an average thickness of about 0.45 mg/cm^2 were evaporated on carbon foils with a thickness of about 40 μg/cm^2 and mounted on a wheel rotating synchronously with the beam macrostructure [20]. The beam energy in the center of the targets was 215.8 MeV, close to the energy of the maximum cross section for the two-neutron evaporation channel of the ^{48}Ca + ^{204}Pb fusion reaction [21].

For separation and collection of evaporation residues in the focal plane detector, TASCA was operated with helium gas at 0.8 mbar pressure and with a magnetic rigidity ($B\rho$) of 2.08 Tm [22,23]. The efficiency of TASCA to guide evaporation residues (ERs) to the focal plane was estimated to be 60% [22,24]. The focal plane detector consisted of a double-sided silicon strip implantation detector (hereafter called the stop detector), with eight additional double-sided silicon strips detectors mounted perpendicular in the backward hemisphere of the stop detector to form a five-sided box configuration. The stop detector comprised 144 vertical (X) and 48 horizontal (Y) strips on the front and back sides, respectively. The focal plane detector was cooled by liquid alcohol circulating at a temperature of $-20\,^{\circ}$C. Signals from the X and Y strips of the stop detector were shaped with preamplifiers with different gains to provide two energy branches up to about 20 and 200 MeV [18]. All amplified and shaped signals were digitized by 100-MHz-sampling FEBEX4 14-bit analog-to-digital converters (ADCs) developed by the GSI experiment electronics department [25,26]. The shape of each signal was stored in 80-μs-long traces. With such long traces, we expect to detect most decays of both the isomeric and the ground state of ^{250}No within the same trace, i.e., in the trace of an implantation signal. Such a measurement was shown to be very efficient for the registration of CEs originating from μs-isomeric states and less dependent on a fine tuning of the low-energy threshold of the stop detector for triggering the data acquisition system [18]. In the present experiment, we used this so-called triggerless CE measurement with a threshold value of $\approx$0.3 MeV. All CEs with energies below this value will be stored in the traces of preceding signals, which initiated the data storage, e.g., the implantation signal of ^{250}No.

Energy resolutions (FWHM) of both X and Y strips were about 40 keV for measurements of external α particles with 5.8 MeV. Energy calibrations were made using α decays of implanted nuclei produced in the "calibration" reaction ^{48}Ca + ^{176}Yb.

A multiwire proportional counter (MWPC) was mounted in front of the focal plane detector and was used to discriminate events passing through TASCA, e.g., evaporation residues (ER) of the compound nucleus ^{252}No.

The average beam intensity on the target was about 4×10^{11} particles per second, which resulted in an average counting rate of about 40 Hz in the stop detector.

III. EXPERIMENTAL RESULTS

We identified a total of 780 fission (FI) events, which were temporally and spatially correlated with implantation signals of their ERs. The time distribution of these events relative to the ER signals is shown in Fig. 1(a). Only thirteen ER-FI events with time differences in the range of 80–250 μs were detected as individual ER and FI signals, i.e., in separate traces. All remaining events were detected as ER-like events having at least two signals in their traces, corresponding to at least the ER and FI.

A. Decays of the long-lived isomeric and the ground states in ^{250}No

Traces of one such ER-like event measured in the X and Y strips are shown in Fig. 2. In this particular case, a small-energy signal between the ER and FI was detected, which we attribute to a CE. A trace from the X strip, which was processed via a high-gain pre-amplifier shows a well-pronounced and well-shaped CE signal, while the high-energy fission signal is saturated. At the same time, a trace from the Y strip shows occurrences of the same signals but with significantly reduced amplitudes because of the low-gain of the preamplifiers, which allows measurement of the full energy of the FI signal. It is important to note that the CE signal is also visible in the Y trace and its time position is the same as in the X trace. This confirms that this small-energy signal is truly associated with the decay of an implanted nucleus, which then fissioned; i.e., it belongs to ^{250}No. Thus, such small energy signals occurring in the same pixel of the stop detector, where ^{250}No was observed to decay by fission, were attributed to originate from the decay of an isomeric state via electromagnetic transitions [18].

In total, 126 ER-FI events were detected with one such a small-energy signal in between the ER and the FI. The time distribution of all ER-FI events detected without and with CE are shown in Figs. 1(b) and 1(c), respectively. It is obvious that the number of counts without CE is significantly reduced

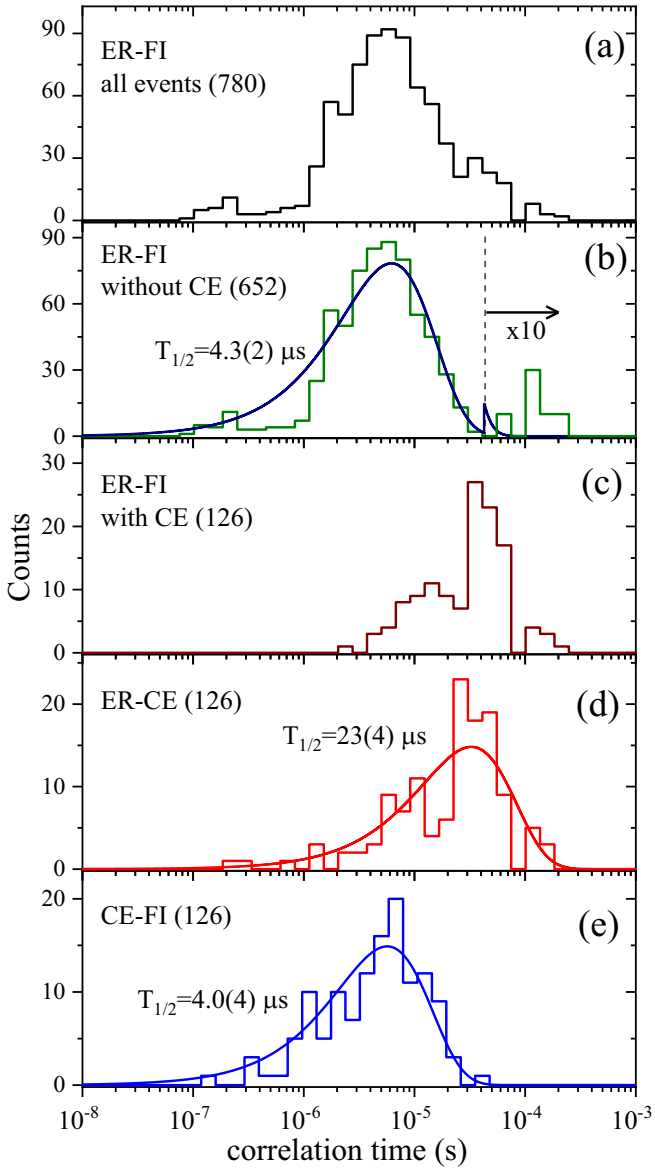

FIG. 1. Time distributions of radioactive decays of species associated with ^{250}No produced in the ^{48}Ca + ^{204}Pb reaction. Time distributions of fission events relative to their implantation signals: (a) all ER-FI, (b) ER-FI events without CE, and (c) ER-FI events with CE (i.e., ER-CE-FI). The number of identified events of each type is given parentheses. Time distributions of (d) CEs relative to preceding ER-signal and (e) FI's relative to CEs, which were observed as ER-CE-FI sequences. Curves represent the calculated time distributions of events according to Ref. [27]. Half-lives extracted from each time distribution are given.

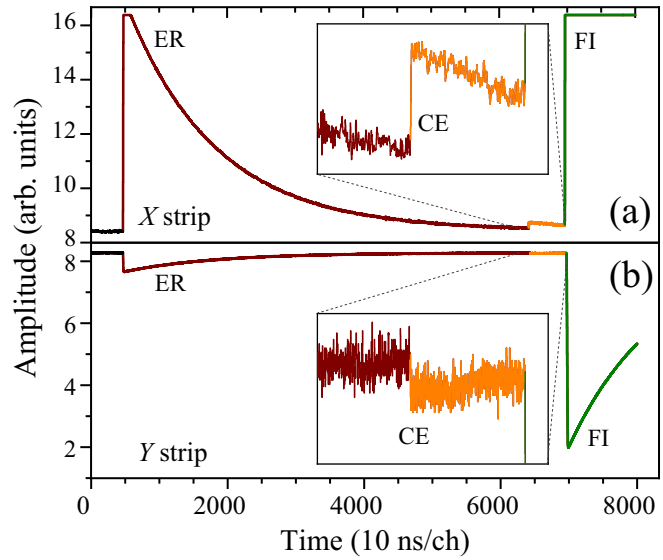

FIG. 2. An example of traces of the implantation signal (ER) correlated with decays of a long-lived isomeric state and ground state in ^{250}No. Signals from X and Y strips are shown in (a) and (b), respectively. Insets show the expanded view of traces in time regions, where low-energy electron signals attributed to decay of an isomeric state were detected.

in the longer time range, which indicates that the contribution of the longer-lived ER-FI component is small. Apparently, this time distribution can be attributed to a single radioactivity and can be described by a time-density function of the radioactive decay curve as given in Ref. [27]. The fit result is shown in Fig. 1(b) and a half-life of 4.3(2) μs was deduced. We note that by comparing shapes of the experimental and the fitted time distributions one can find that some ER-FI events in the time range of 0.2–1.0 μs may be missing. This may be due to missing signals from a few nonfunctioning Y strips. Without traces from the Y strip, the identification relies exclusively on the X trace, where signals from ER and FI events often result in a single saturated signal. Such a signal cannot be identified as an ER-FI sequence. In the present work, such a full saturation seemingly occurred preferentially within ≈ 1 μs [28,29]. We also note that almost no event was detected between 75 and 100 μs. This could be due to the busy time of the data acquisition system, which is needed to store a large amount of 80-μs-trace data. However, such "missing" events in the time distributions will not affect the extracted physics quantities and discussions substantially.

The time distribution of ER-FI events with CE [see Fig. 1(c)] shows the presence of a long-lived activity, which has to be disentangled into two ER-CE and CE-FI components. Accordingly, the time distributions of CE and FI signals relative to their preceding (ER and CE, respectively) ones are shown in Figs. 1(d) and 1(e). These time distributions clearly reveal two different radioactive decays with different half-lives. Decay of the longer-lived state is strongly associated with the emission of CEs and with the population of a short-lived state, which fissions.

Fits of these time distributions describe the experimental data well and result in half-lives of 23(4) and 4.0(4) μs. A half-life of 4.0(4) μs of the CE-FI events agrees perfectly with the one deduced from ER-FI events without CE. Thus, these two activities belong to the decay of the same, i.e., ground state in ^{250}No. The longer-lived activity corresponds to the decay of the isomeric state. These assignments are in fine agreement with previously reported results [14–16]. However, the presently measured half-life of 23(4) μs for

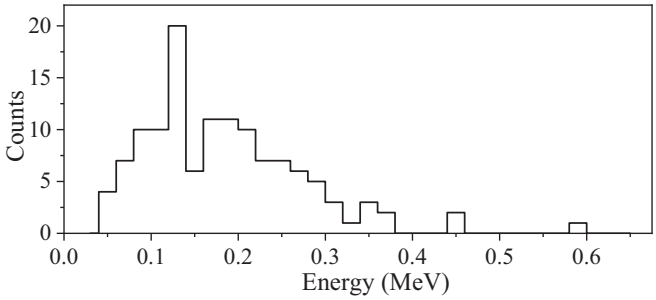

FIG. 3. Energy spectrum of CE signals found in the ER-CE-FI sequences.

the isomeric state is somewhat shorter than any other previously reported one: 43^{+22}_{-15} μs from Ref. [14], 36(3) μs from Ref. [15], $34.9^{+3.9}_{-3.2}$ μs from Ref. [16]. By taking into account our measured time distributions of radioactive decays and the fine results of the fits (see Fig. 1), we do not find a reasonable explanation for this. Thus, we attribute it to a statistical fluctuation. The present half-lives of 23(4) and 4.0(4) μs were deduced from the time distributions of ER-CE-FI events, which should exclude any disturbance due to the presence of contamination.

The energy spectrum of CEs registered in between ER and FI is shown in Fig. 3. Most CEs have energies below the threshold value of ≈0.3 MeV and were recorded in traces of ERs. In addition, some CEs with energies larger than the ≈0.3 MeV which initiated the data storage have also been detected. The present energy spectrum is in agreement with previously measured data [16].

B. Evidence for a higher-lying second isomeric state

In addition to 126 ER-CE-FI sequences, two FI events with two CEs between the ER and FI signals were found. Traces of the *X* strips of these two ER-CE_1-CE_2-FI events are shown in Fig. 4. In both cases, all four signals were stored in a single 80 μs trace and are also seen in the corresponding traces from the *Y* strips, which shows that they are all spatially correlated.

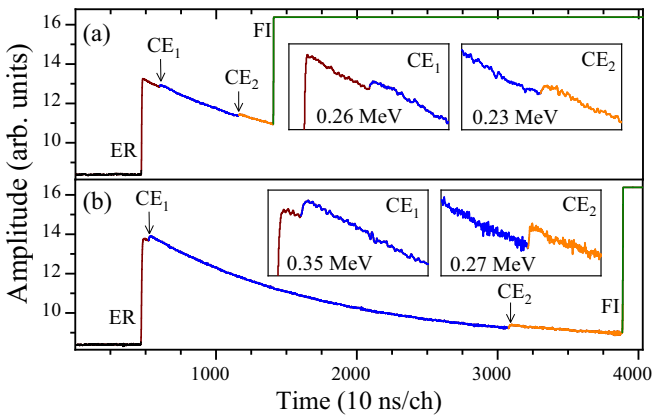

FIG. 4. *X*-strip traces of two ER-CE_1-CE_2-FI events. Insets show close look of regions where CEs were detected. Energies of CEs are given.

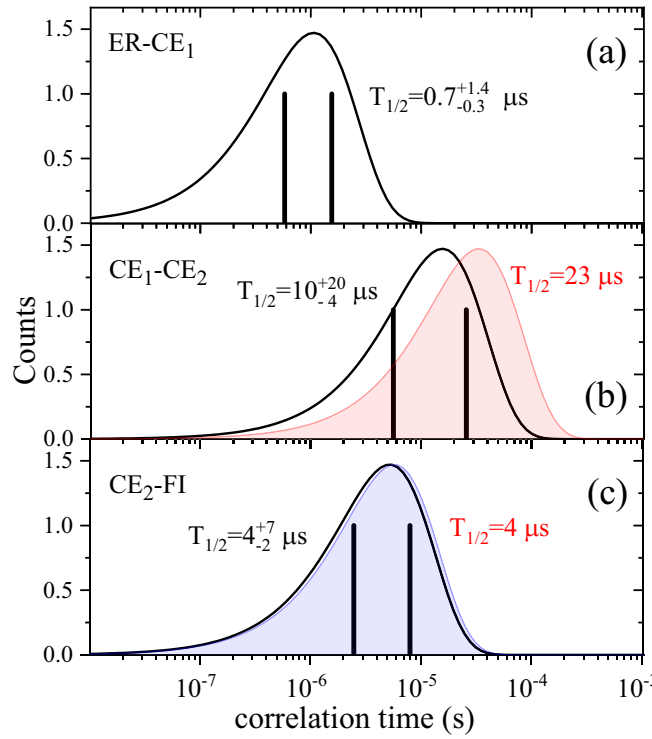

FIG. 5. Correlation times of the CE_1, CE_2, and FI events relative to the preceding events. Curves represent the calculated time distributions of each pair according to Ref. [27]. Shaded curves correspond to the calculated time distributions of the long-lived isomeric state and the ground state. See text for details.

Such ER-CE_1-CE_2-FI events were observed in our previous works [18,30], e.g., in ^{256}Rf. There they were attributed to the deexcitation of a higher-lying *K* isomeric state that proceeds via the population of a lower-lying *K* isomeric state. Accordingly, the present two events are also attributed to such a case.

The correlation times of the CE_1, CE_2, and FI events relative to their preceding signals in the ER-CE_1-CE_2-FI sequence are shown in Fig. 5. The time distribution curves calculated with the average values of each pair are also shown. Since the last two members of the sequences might correspond to the decays of the ground and long-lived isomeric states of ^{250}No, the calculated time distributions of these states are also shown in Fig. 5. The average half-lives of the FI and the CE_2 events agree well with the presently measured half-lives of the ground and the long-lived isomeric states of ^{250}No, respectively. Accordingly, the last two members in both ER-CE_1-CE_2-FI sequences are attributed to the decays of the long-lived isomeric state, which was populated in the decay of another, higher-lying isomeric state, the deexcitation of which is detected by its CE_1. A half-life of $0.7^{+1.4}_{-0.3}$ μs was deduced for this second isomeric state, shorter than the other two states in ^{250}No and comparable with the flight time (≈0.6 μs) of ERs through TASCA. The latter leads to the expectation of in-flight decay of at least two further cases, in which CE_1 was not detected. However, these cases will still be detected as a ER-CE_2-FI sequence, thus they will be identified in Fig. 1(c)

and attributed to the decay of the long-lived isomeric state (hereafter ^{250m1}No).

On the other hand, this short-lived and higher-lying isomeric state (hereafter ^{250m2}No) may have other de-excitation branches. Let us consider two scenarios by assuming that the short-lived isomer has survived the flight through TASCA. First, it may fission directly, which will result in ER-FI correlations with a half-life of ≈0.7 μs that may be found in Fig. 1(b). However, the presence of such ER-FI events cannot be examined because of the large contribution of ER-FI events of the ground state.

The second scenario is that ^{250m2}No decays to the ground state without passing through ^{250m1}No. In such a case its decay will be detected as ER-CE$_1$-FI events in the data shown in Fig. 1(c). The potential presence of such events can only be examined in Fig. 1(d), where the CEs with an average half-life of ≈0.7 μs would be found. We observed six CEs with correlation times of shorter than 2 μs, which, however, fit well in the time distribution of ^{250m1}No. Therefore, these six events were not attributed to the decay of the higher-lying isomeric state.

Finally, based on the present data and analyses, we attribute only the deexcitation via the lower-lying ^{250m1}No state to the decay of the higher-lying isomeric state. For the population probability of this higher-lying isomeric state we give an upper limit of 1%.

C. Search for direct fission from ^{250m1}No

In the present data, an ER-FI event corresponding to the direct fission of ^{250m1}No should be detected without CE and with a long correlation time. Such events have to be sought in the data shown in Fig. 1(b), in the region where the contribution of the short-lived ground-state component is negligible.

In order to exclude an effect of the short-lived ground-state component, we consider the fission events with relatively long correlation times, i.e., $>$ 40 μs, where only one fission event from the ground state is expected. This was calculated with the fitted time-density function of the 4.3-μs activity and with the number of events within the range of up to 40 μs which were attributed to the 4.3-μs activity [see Fig. 1(b)].

Six ER-FI events with correlation times in the range 40–200 μs were observed. One of these six events, which has the shortest correlation time ($<$100 μs), is attributed to it belonging to the short-lived component. At the same time, the time range of 40–200 μs covers about 30% of the full time-density function of the 23-μs activity [cf. Figs. 1(b) and 1(d)]. Accordingly, the remaining five ER-FI events could originate from the direct fission of ^{250m1}No.

On the other hand, these events still could belong to the electromagnetic decay of ^{250m1}No, i.e., to the data shown in Fig. 1(c) if their CE signals remained undetected.

These five events were stored in the data as an individual fission signal with no CE signal prior to the FI signal up to ≈4.7 μs, which is the time prior to the trigger (see Fig. 2). However, if the CE from ^{250m1}No is emitted with an energy that is smaller than the threshold value of 0.3 MeV and with lifetimes longer than 4.7 μs before the detection of the FI signal, then such a CE will not be detected in the trace of the

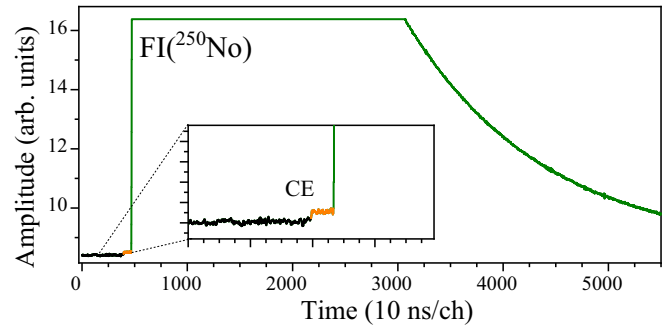

FIG. 6. An example of a trace (X strip) of a FI event, where the CE was detected prior to the FI signal. The inset shows the expanded view of the trace in the time region where the CE signal was detected.

FI signal. Therefore, in the present data the pretrigger time of ≈4.7 μs is the main reason for the loss of CEs for these cases. Accordingly, the above-mentioned five ER-FI events could be misassigned if their CE signals were not recorded. To examine this possibility, we have to estimate the expected number of ER-CE-FI events detected without their CEs, which could be falsely assigned to be long-lived ER-FI events.

In total, eight out of thirteen events where ER and FI signals were stored in individual traces were found to be ER-CE-FI events [see Figs. 1(c) and (d)] with the CE and FI signals in the same traces. One example of such a CE-FI case is shown in Fig. 6. The time distribution of these eight FI events relative to their CE is shown in Fig. 7. Among them, in one case with a correlation time of 5.43 μs the CE energy was sufficient to trigger data storage. The other seven CE energies were smaller than 0.3 MeV, thus they were detected within the ≈4.7 μs pretrigger time of FI traces. Since all these FI events should belong to the decay of the ground state in ^{250}No, their time distribution should reveal the 4.0-μs activity as in Fig. 1(e).

Based on the observed seven CE-FI events with correlation times smaller than 4.7 μs and the calculated time distribution of a 4.0-μs activity [27], we estimated that six CE-FI events

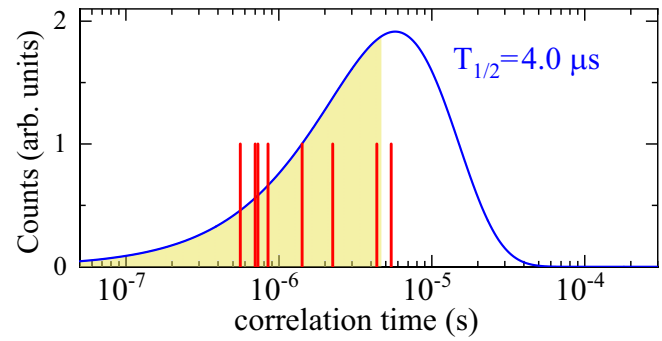

FIG. 7. The time distribution of eight FI events relative to the preceding CE signal in their traces. The time-density function curve for the 4.0-μs activity, which describes the time distribution of ER-FI events without CE shown in Fig. 1(b), is given, and its shaded region corresponds to ≈50% probability nof observing the FI events with correlation times up to ≈4.7 μs. See text for details.

are expected to be detected with correlation times longer than 4.7 μs. We observed only one event with a correlation time of longer than 4.7 μs, which would mean that the five CE-FI events should be stored in the data as single FI events. Accordingly, in the data we should observe five FI events, which are artificially forming the long-lived ER-FI correlation without CE, while their true origin is the ER-CE-FI sequence. This expected number is in perfect agreement with the above-discussed five long-lived ER-FI events detected without CE [see Fig. 1(b)]. Therefore, they are attributed to originate from the decay of the ground state, fed from ^{250m1}No via electromagnetic transition.

Finally, we conclude that in the present data no unambiguous evidence for a direct fission of the long-lived isomeric state within 40–200 μs is observed. However, we do not exclude that the direct fission may have occurred in the time range of shorter than 40 μs, where the probability to observe the 23-μs activity is two times larger than in the above-used time range. We attribute two of all ER-FI events, which were assigned to ground-state decay of ^{250}No and with correlation times up to 40 μs, to this scenario, i.e., as being ER-FI(^{250m1}No).

Accordingly, this results in two ER-FI events out of in total 133 (126 + 2 + 5; see above and previous paragraphs) decays from ^{250m1}No. This results in a direct fission branching of ^{250m1}No of $0.015^{+0.020}_{-0.005}$. Asymmetric errors corresponding to two events were calculated according to Ref. [27] and they cover a confidence interval of 68%. However, experimentally no ER-FI event that can be unambiguously assigned to fission from ^{250m1}No was observed. Thus, as a final result, only an upper limit of 0.035 from the above value can be attributed to the direct fission branching of ^{250m1}No.

IV. DISCUSSION OF THE EXPERIMENTAL RESULTS

From a total of 780 ER-FI events, a total production cross section of 32(2) nb is deduced. Out of these, <1%, 17(3)%, and 83(3)% populate the higher-lying ^{250m2}No, the lower-lying ^{250m1}No, and the ground state, respectively.

A. Fission from the long-lived isomeric state

From our data, a fission branch of the long-lived K-isomeric state ^{250m1}No was found to be a factor of at least 164 times smaller than that of the ground state. This value is significantly larger than the previously given one of 19 [16].

Such an enhanced fission stability should originate from the configuration of quasiparticles (qps) and the level density of the nucleus, which in turn determines the decay of the high-K state via electromagnetic transitions. The exact qp configuration of the long-lived K-isomeric state in ^{250}No is still unknown. According to most theoretical predictions (e.g., [12,14,16] and references therein), this state is most probably formed by the coupling of the spin-up $\nu 5/2^+[622]$ and the spin-down $\nu 7/2^+[624]$ orbitals, which results in $K^\pi = 6^+$. Such a state is known to occur in the lighter ^{242}Pu and ^{244}Cm isotones. Moreover, recently, an experimental signature for $K^\pi = 6^+$ has been obtained for ^{250}No in Ref. [31] and an excitation energy of ≈1.25 MeV was estimated for ^{250m1}No. Our measured population probability value of 17(3)% is similar to values known for the 2-qp K-isomeric states in ^{252}No (≈ 50% [32]), ^{254}No (28(2)% [33]), ^{254}Rf (≈ 25% [17], 16(5)% [34]) and ^{256}Rf (≈ 18% [18]), which supports a 2-qp origin of ^{250m1}No.

We note that the above deduced factor of greater than 164 is just the ratio of fission branches of the K-isomeric state and of the ground state, which, however, does not quantify and reflect the true physical process that retards fission from an excited state. It is well known that the fission probability increases as a function of excitation energy [7]. In the absence of a hindrance caused by the K quantum number, fission from a highly excited state, e.g., at a typical energy above 1 MeV, should be faster than fission from the ground state [35]. Accordingly, the effect of the K quantum number on fission would better be discussed relative to fission of a virtual $K = 0$ state at the same excitation energy. For this, one should calculate the fission half-life of the virtual $K = 0$ state by taking into account only the excitation energy and the fission barrier height. However, such values are missing in theoretical works, where the fission process is qualitatively described on the multidimensional potential energy surface. Therefore, here, we will use a simple semiempirical approach.

Recently, it has been shown that fission of an excited nucleus can be described with a different fission-barrier shape compared to that at its ground state [35]. Nuclei around ^{250}No still have a double-humped fission barrier [7,36,37]. In a recent analysis of the effective width, i.e., the curvature energy of the fission barriers based on all known spontaneous fission half-lives of even-even nuclei [30], it has been suggested that ^{250}No seemingly has no outer barrier, which in contrast is present in the heavier isotopes with neutron numbers around 152 [37]. Accordingly, one can assume that the fission-barrier shape in this nucleus does not significantly change with an increase of the excitation energy, i.e., it remains singly humped [35]. In this case, a parabolic barrier should be a good approximation for ^{250}No, and one can estimate the fission half-life of the virtual $K = 0$ state by using the Hill-Wheeler formula [38]. According to Ref. [30], by using the fission-barrier height of 5.83 MeV from Ref. [36] for ^{250}No, an effective fission-barrier width of 1.82 MeV, and an excitation energy of ≈1.25 MeV, the fission half-life of the virtual $K = 0$ state is calculated to be ≈0.05 μs. Now, by comparing this value with the present experimental lower limit of the fission half-life of 657 μs, a factor of larger than 1.3×10^4 can be attributed as hindrance of the fission process due to the $K = 6$ qp configuration in ^{250m1}No. Indeed, this (arguably theory-dependent) estimate appears reasonable in this case of a likely singly humped barrier. However, such an estimate is not much effected by the chosen value of the fission barrier height if the corresponding theoretical approach describes the experimental fission half-life tendencies well, as discussed in Ref. [30]. For instance, by taking the different theoretical fission barrier height value of 6.14 MeV from Ref. [39] one calculates an effective parabolic fission-barrier width of 1.91 MeV for the ground state of ^{250}No. Then, the fission half-life of the virtual $K = 0$ state, calculated similarly as above, is 0.07 μs, which results in a hindrance factor of larger than 0.94×10^4. As one can see, the variation of the

absolute value of the fission barrier height does not affect the order of magnitude of the estimated fission hindrance.

On the other hand, recently [40,41], the measured fission half-lives from the $1/2^+[631]$ and $7/2^+[624]$ states in ^{253}Rf have allowed isolation of the fission hindrance due to the single-particle-orbital effect. In Ref. [40], the fission half-lives of these states are different by a factor of ≈ 330, which has been attributed to an effect of $\Delta K = 3$ on the fission process. Simply, by assuming that the present isomeric state has $K = 6$, the rough estimate of $330 \times 330 \approx 10^5$ follows, which is of a similar order of magnitude as the above value. Recently, a fission hindrance of 120 due to the effect of $\Delta K = 3$ has been extracted similarly in ^{247}Md [42]. The use of this value results in $\approx 1.4 \times 10^4$, which is again in line with the above discussion. Therefore, such an estimate also seems to be a reasonable way of discussing fission hindrance.

As conclusion of the above discussions, we extracted a hindrance factor of greater than 10^4 for fission of ^{250m1}No due to the K quantum number. Such a large hindrance value is also supported by theoretical predictions in which the influence of the K quantum number on fission is usually expressed via an increase of the fission-barrier height and a change in shape compared to the ground state [8,43]. For instance according to the theoretical calculations made in Ref. [43], the fission-barrier height of the K-isomeric state in ^{250}No, i.e., ^{250m1}No, was predicted to be increased by 1.44 MeV compared to the height of the ground-state fission barrier. By taking into account the excitation energy of $\approx$1.25 MeV ($<$1.44 MeV) [31], ^{250m1}No is still predicted to overcome a larger fission barrier, i.e., to be more stable against fission than the ground state.

B. The short-lived isomeric state

Despite the limited experimental data on the short-lived isomeric state, some rough discussion of its properties can be made.

First, the deexcitation of ^{250m2}No into ^{250m1}No indicates that its origin is also due to a high-K quantum number. This isomer should be located at an excitation energy, which is at least 0.3 MeV above ^{250m1}No. This value is the average energy of the two CEs (see Fig. 4). Similarly to the discussions made above for ^{250m1}No, a fission half-life of 0.02 μs is calculated for a virtual $K = 0$ state in ^{250}No with a fission barrier height of 5.83 MeV from Ref. [36] but with an excitation energy of 1.55 MeV. Now, if we apply the fission-hindrance lower limit of 10^4 extracted from ^{250m1}No, then a fission half-life of longer than 200 μs is expected for ^{250m2}No. In this case, direct fission of ^{250m2}No, which we sought in the data (see Sec. III B) should not be detected within the present low statistics.

The population probability of ^{250m2}No is found to be much lower than the one for the 2-qp ^{250m1}No state. This can be due to a significantly higher excitation energy and significantly different qp configuration of ^{250m2}No compared to ^{250m1}No. These are typically associated with K isomeric states, which are formed in couplings of 4 qps [18]. Isomeric states having presumably 4-qp origin and thus being located above the 2-qp ones are known in the heavier isotope ^{254}No [33]. It seems that occurrences of multiple high-K isomeric states in a particular nucleus, which are also known in ^{254}Rf [17] and ^{256}Rf [18,44,45], are a widespread phenomenon in this region of deformed heavy nuclei.

V. SUMMARY AND CONCLUSION

In the present work, we detected and investigated 780 decays of ^{250}No. In 126 cases, decay of the long-lived isomeric state via electromagnetic transitions with a half-life of 23(4) μs was measured by detecting conversion electrons. No fission from this isomeric state was observed. Rather, it deexcites into the spontaneously fissioning ground state, which has a half-life of 4.0(4) μs. An upper limit of 0.035 for the fission branching of the long-lived isomeric state in ^{250}No was obtained, corresponding to a fission half-life of longer than 657 μs. This is more than 164 times longer than the one of the ground state. It is evident that the high K quantum number strongly retards the fission process. The effect of the high-K value was discussed in connection with semi-empirical calculations and related experimental observations. According to these discussions, a suggested assignment of $K = 6$ [31] of the long-lived isomeric state in ^{250}No should hinder its fission by a large factor, i.e., at least by a factor of 10^4.

We observed evidence of a hitherto unknown higher-lying short-lived isomeric state with a half-life of $0.7^{+1.4}_{-0.3}$ μs. Two events were attributed to the decay of this isomeric state. They deexcite via the population of the lower-lying and longer-lived isomeric state.

Occurrences of multi-quasiparticle high-K isomeric states, as predicted by theory, seem to be a widespread feature in the heavy nuclei in this region, but their production rates are low. The presently used triggerless conversion electron measurement based on fast digital electronics is well suited for the search of similar states in neighboring and heavier even-even nuclei.

ACKNOWLEDGMENTS

We are grateful to GSI's ion-source and UNILAC staff, the Target Laboratory, and the Experiment Electronics department for their support of the experiment. The results presented here are based on the experiment U308, which was performed in 2018 at the beam line X8/TASCA at the GSI Helmholtzzentrum für Schwerionenforschung, Darmstadt (Germany) in the frame of FAIR Phase-0.

[1] D. Ackermann and C. Theisen, Phys. Scr. **92**, 083002 (2017).
[2] P. Walker and F. R. Xu, Phys. Scr. **91**, 013010 (2016).
[3] G. Dracoulis *et al.*, Rep. Prog. Phys. **79**, 076301 (2016).
[4] M. Asai, F. P. Heßberger, and A. Lopez-Martens, Nucl. Phys. A **944**, 308 (2015).
[5] F. Kondev, G. Dracoulis, and T. Kibédi, At. Data Nucl. Data Tables **103-104**, 50 (2015).
[6] K. Löbner, Phys. Lett. B **26**, 369 (1968).
[7] R. Vandenbosch and J. R. Huizenga, *Nuclear Fission* (Academic, New York and London, 1973)

[8] F. R. Xu, E. G. Zhao, R. Wyss, and P. M. Walker, Phys. Rev. Lett. **92**, 252501 (2004).
[9] P. Jachimowicz, M. Kowal, and J. Skalski, Phys. Rev. C **83**, 054302 (2011).
[10] H. L. Liu, P. M. Walker, and F. R. Xu, Phys. Rev. C **89**, 044304 (2014).
[11] P. Jachimowicz, M. Kowal, and J. Skalski, Phys. Rev. C **98**, 014320 (2018).
[12] G. G. Adamian, N. V. Antonenko, and W. Scheid, Phys. Rev. C **81**, 024320 (2010).
[13] S. Hofmann, F. P. Heßberger *et al.*, Eur. Phys. J. A **10**, 5 (2001).
[14] D. Peterson, B. B. Back, R. V. F. Janssens, T. L. Khoo, C. J. Lister, D. Seweryniak, I. Ahmad, M. P. Carpenter, C. N. Davids, A. A. Hecht, C. L. Jiang, T. Lauritsen, X. Wang, S. Zhu, F. G. Kondev, A. Heinz, J. Qian, R. Winkler, P. Chowdhury, S. K. Tandel *et al.*, Phys. Rev. C **74**, 014316 (2006).
[15] A. Svirikhin *et al.*, Phys. Part. Nuclei Lett. **14**, 571 (2017).
[16] J. Kallunkathariyil *et al.*, Phys. Rev. C **101**, 011301(R) (2020).
[17] H. M. David *et al.*, Phys. Rev. Lett. **115**, 132502 (2015).
[18] J. Khuyagbaatar *et al.*, Phys. Rev. C **103**, 064303 (2021).
[19] A. Semchenkov *et al.*, Nucl. Instrum. Methods Phys. Res., Sect. B **266**, 4153 (2008).
[20] E. Jäger *et al.*, J. Radiol. Nucl. Chem. **299**, 1073 (2014).
[21] Y. T. Oganessian, V. K. Utyonkov, Y. V. Lobanov, F. S. Abdullin, A. N. Polyakov, I. V. Shirokovsky, Y. S. Tsyganov, A. N. Mezentsev, S. Iliev, V. G. Subbotin, A. M. Sukhov, K. Subotic, O. V. Ivanov, A. N. Voinov, V. I. Zagrebaev, K. J. Moody, J. F. Wild, N. J. Stoyer, M. A. Stoyer, and R. W. Lougheed, Phys. Rev. C **64**, 054606 (2001).
[22] J. Khuyagbaatar *et al.*, Nucl. Instrum. Methods Phys. Res., Sect. A **689**, 40 (2012).
[23] J. Khuyagbaatar, V. P. Shevelko, A. Borschevsky, C. E. Dullmann, I. Y. Tolstikhina, and A. Yakushev, Phys. Rev. A **88**, 042703 (2013).
[24] K. E. Gregorich, Nucl. Instrum. Methods Phys. Res., Sect. A **711**, 47 (2013).
[25] N. Kurz *et al.*, GSI Scientific Report 2011 [GSI Report 2012-1] (GSI Darmstadt, 2012), Vol. 2012-1, p. 252, https://repository.gsi.de/record/53520/files/GSI-Report-2012-1.pdf.
[26] https://www.gsi.de/work/forschung/experimentelektronik
[27] K. H. Schmidt *et al.*, Z. Phys. A **316**, 19 (1984).
[28] J. Khuyagbaatar *et al.*, EPJ Web Conf. **131**, 03003 (2016).
[29] J. Khuyagbaatar *et al.*, Phys. Rev. Lett. **125**, 142504 (2020).
[30] J. Khuyagbaatar, Nucl. Phys. A **1002**, 121958 (2020).
[31] M. Tezekbayeva *et al.*, Eurasian J. Phys. Funct. Mater. **3**, 300 (2019).
[32] B. Sulignano *et al.*, Eur. Phys. J. A **33**, 327 (2007).
[33] F. P. Heßberger *et al.*, Eur. Phys. J. A **43**, 55 (2010).
[34] J. Khuyagbaatar *et al.*, Nucl. Phys. A **994**, 121662 (2020).
[35] J. Khuyagbaatar, Eur. Phys. J. A **55**, 134 (2019).
[36] P. Moller *et al.*, At. Data Nucl. Data Tables **59**, 185 (1995).
[37] R. Rodríguez-Guzmán and L. M. Robledo, Phys. Rev. C **98**, 034308 (2018).
[38] D. L. Hill and J. A. Wheeler, Phys. Rev. **89**, 1102 (1953).
[39] P. Jachimowicz, M. Kowal, and J. Skalski, Phys. Rev. C **95**, 014303 (2017).
[40] J. Khuyagbaatar *et al.*, Phys. Rev. C **104**, L031303 (2021).
[41] A. Lopez-Martens *et al.*, Phys. Rev. C **105**, L021306 (2022).
[42] F. P. Heßberger *et al.*, Eur. Phys. J. A **58**, 11 (2022).
[43] P. M. Walker, F. R. Xu, H. L. Liu, and Y. Sun, J. Phys. G: Nucl. Part. Phys. **39**, 105106 (2012).
[44] H. B. Jeppesen *et al.*, Phys. Rev. C **79**, 031303(R) (2009).
[45] A. P. Robinson *et al.*, Phys. Rev. C **83**, 064311 (2011).